ORIGINAL PAPER

RJME
Romanian Journal of Morphology & Embryology
http://www.rjme.ro/

Comparison of pathology, blood gas and biomarkers between two rat models of acute lung injury

YUAN-DONG HU[1)], LING JIANG[2)], LIU-LIN XIONG[1)], YUE HU[3)], QING-JIE XIA[4)], TING-HUA WANG[1,4)]

[1)]*Department of Anesthesiology, West China Hospital, Sichuan University, Chengdu, China*
[2)]*Department of Anesthesiology, People's Hospital of Guizhou Province, Guizhou University, Guiyang, China*
[3)]*Department of Anesthesiology, First People's Hospital of Shuangliu District of Chengdu, Chengdu, China*
[4)]*Institute of Neurological Disease, West China Hospital, Sichuan University, Chengdu, China*

Abstract

An ideal animal model to explore pathogenesis and prevention of acute lung injury (ALI) is essential. The present study aims to compare the difference in pathology, blood gas values and biomarkers of two acute lung injury rat models at different time intervals. In the experiment, rats were randomly divided into three groups: lipopolysaccharide (LPS) group, oleic acid (OA) group and control group. Changes of pathology, blood gas values and blood–air barrier biomarkers were analyzed at 15 minutes, 6 hours, 12 hours and 24 hours after injection. The results showed that the two models exhibited different features. Compared with the LPS rats, OA rats exhibited significantly severe pathological changes, lower arterial oxygen partial pressure (PaO_2) value and higher level of injury biomarkers. However, LPS rats boasted greater lactic acid (LAC) level and more severe acidosis than OA rats. This study suggests that LPS-induced model has greater value in researches on microcirculation dysfunction and sepsis resulting from ALI, while OA-induced model has greater repeatability in area of gas exchanging after ALI. These events may provide a new theoretical evidence for the model establishment of ALI.

Keywords: acute lung injury, lipopolysaccharide, oleic acid, blood gas, blood–air barrier.

Introduction

Acute lung injury (ALI), as a major clinical complication, is followed by high rate of morbidity and mortality [1]. Although intensive efforts have been made, there are still no effective therapies [2]. One of the most important reasons is that models are not perfect and they can hardly imitate the pathologic change. A large number of substances are employed to establish ALI model including lipopolysaccharide (LPS), oleic acid (OA; *cis*-9-octadecenoic acid), bleomycin, hydrochloric acid, chloroquine, seawater, etc. Among these substances, LPS and OA are two of the most popular substances to establish animal model [3].

Traditionally, LPS-induced model was developed to mimic ALI caused by sepsis [4], while OA-induced model was used to simulate ALI after a long bone trauma [5]. However, some questions were raised after reviewing related literatures. Firstly, the difference of their capability to impair the blood-air barrier, which is the physiological basis of gas exchange, has not been fully compared. Furthermore, the value of arterial oxygen partial pressure (PaO_2), which is the primary clinical index of ALI [6], was absent in a large part of studies. Besides, a majority of researches focused on situation of animals only at a single time point, while ALI may have very unique physiological performance at different phases of diseases.

Therefore, we conducted this study to compare the two models according to appearance, wet/dry (W/D) ratio, morphology, blood gas parameters and cell biomarkers at four time points. We hope to draw a clearer picture of their characteristics and have a better understanding of their inner mechanism.

Materials and Methods

Animals and experimental design

The study protocol was approved by the Institutional Animal Care and Use Committee of Sichuan Province, China. Animals (9-week-old; 230/270 g body weight; females; specific pathogen-free Sprague–Dawley rats; purchased from Dossy Experimental Animals Co., Ltd., Chengdu, China) were maintained under standard housing conditions. All experiments on animals were carried out in an ethical manner. Four time points were set: 15 minutes, 6 hours, 12 hours and 24 hours post-injection. Each time point contained three groups including control group, LPS group and OA group (every time point, n=6 for each group). After an adaptive phase of 1–2 days, rats were injected with 0.1 mL/kg oleic acid (Sigma-Aldrich 01008, emulsified in blood prior) or 10 mg/kg LPS respectively (*Escherichia coli* 055:B5, Sigma-Aldrich L2880). Then, each animal received drug dissolved in sterile physiological saline to 0.5 mL through the tail vein. The control group received only 0.5 mL saline injection. Rats were sacrificed at 15 minutes, 6 hours, 12 hours and 24 hours after administration.

Blood and lung tissues harvest

Rats were anaesthetized with intraperitoneal 3.6% chloral hydrate (10 mL/kg). Later, their abdomens were quickly open, and the blood samples were obtained from the aortic artery, by a syringe pretreated with 100 U/mL heparin. Then, they were sent immediately for blood gas analysis. Subsequently, animals were sacrificed by abdominal aorta exsanguination. During the process, the

incision extended to chest to expose the lung, and the left lung was removed after ligation of left hilus. Followed by lavage from right ventricle to left atrium with cold phosphate-buffered saline (PBS), under a constant pressure of 55 cmH_2O, the upper lobe of right lung tissue was snap frozen in liquid nitrogen and stored at -80^{0}C for real-time quantitative polymerase chain reaction (PCR) assays. Bronchoalveolar lavage was then performed with cold 4% paraformaldehyde, under a constant pressure of 25 cmH_2O. And then the lower lobe of right lung was removed and fixed for Hematoxylin–Eosin (HE) staining. No mechanical ventilation was used during the experiment. The surgery duration was kept within 10 minutes.

The wet/dry weight ratio of lung tissue

The left lung of each animal was weighed immediately after excision as described above. Lung tissues were dried in a drying oven at 60^{0}C for 24 hours and weighed again. The wet/dry ratio of the lung was calculated as W/D ratio = $weight_{wet}/weight_{dry} \times 100\%$ [7].

Real-time quantitative PCR

The lung tissues were homogenized in 1 mL of TRIzol Reagent (SuperfecTRI™, Shanghai, China) prior to complementary DNA (cDNA) synthesis. Reverse transcription to cDNA was executed according to the instruction of RevertAid First Strand cDNA Synthesis Kit (Thermo Scientific, Massachusetts, USA). Simply, single-stranded cDNAs were synthesized by incubating template RNA (2.5 μg) with oligo-(dT) 18 primer (1 μL), and water, nuclease-free (to 12 μL) at 65^{0}C for 5 minutes in a volume of 12 μL, followed by mixing RevertAid M-MuLV Reverse Transcriptase (200 U/μL, 1 μL) with 5× reaction buffer (4 μL), RiboLock RNase Inhibitor (20 U/μL, 1 μL), and 10 mM deoxy-nucleotide triphosphate (dNTP) Mix (2 μL), by incubating for 60 minutes at 42^{0}C, in a final volume of 20 μL. The reaction was terminated by heat at 70^{0}C for 5 minutes. PCR was operated using CFX96™ Thermal Cycler (BIORAD, California, USA). Five μL of five-fold diluted template cDNA was added in each system with a final volume of 25 μL. Sequences information was listed in Table 1.

Table 1 – ***The detailed information on primers for RT-PCR***

Gene	Sequence (5'-3')	Annealing temperature [^{0}C]
β-Actin	F: GAAGATCAAGATCATTGCTCCT R: TACTCCTGCTTGCTGATCCA TM: CTGTCCACCTTCCAGCAGA	53
AGER	F: CCACCAAGATCCCAGTGAT R: GAAGGCTTGGTTAGCATTGAG TM: CTGCCCGTCCTGGACAAGAC	53
MUC1	F: GACACCTACCATCCTATGAG R:CTGCCATTGCCTGTCGAAACCT TM: CTACCTACCACACTCACGGAC	55
vWF	F: GACACTTGCTCCTGTGAGT R: ACAGCTCTGGGGGCACAGT TM: CTGCCTATGCCCACGTGTG	53
LAM5	F: CCACGTCATTGGCCGTGACT R: GTGAGCTCGTCACACAGGCG TM: CCAACTGCAGGCCCTGTGAC	57

RT-PCR: Reverse transcription–polymerase chain reaction; AGER: Advanced glycosylation end product-specific receptor; MUC1: Mucin 1; vWF: von Willebrand factor; LAMA5: Laminin subunit alpha-5; F: Forward primer; R: Reverse primer; TM: Terminal sequence.

PCR amplification was carried out as follows: initial denaturation: 94^{0}C, 5 minutes; denaturation: 94^{0}C, one minute; annealing: annealing temperature, one minute; elongation: 72^{0}C, one minute (denaturation, annealing, extending three walk 35 cycles); total elongation: 72^{0}C, 10 minutes. Relative gene expression was calculated by using the $2^{-\Delta\Delta Ct}$ method and *β*-actin was employed as endogenous control gene.

HE staining

The lower lobe of right lung was fixed in 4% para-formaldehyde, embedded in paraffin and HE stained. Three sections of each animal were selected for HE staining. Subsequently, all sections (400×, 10 microscopic fields of each section) were examined and graded by a pathologist who was blind with the experimental condition. Briefly, the sections were assessed with the airway epithelial necrosis, intra-alveolar edema, hyaline membranes, hemorrhage and recruitment of inflammatory cells to the air spaces. And then each characteristic was scored by a semi-quantitative scoring system [8]. Edema, alveolar and interstitial inflammation, alveolar and interstitial hemorrhage, atelectasis, and hyaline membrane formation were respectively scored on a scale of 0 to 4: no injury – score of 0; injury in 25% of the field – score of 1; injury in 50% of the field – score of 2; injury in 75% of the field – score of 3; and injury throughout the field – score of 4. Ten microscopic fields from each slide were analyzed. The sums of tissue slides were averaged for the evaluation of severity of lung injury.

Statistical methods

Results were presented as means ± standard error of mean (SEM). The differences were assessed by virtue of one-way analysis of variance (ANOVA). Statistical analysis was performed with Predictive Analytics Software (PASW) Statistics 18 (IBM SPSS Inc.) and $p<0.05$ was considered as statistical significance.

Results

Appearance

Six hours after injection, the lower lobes of right lung were obtained. As shown in Figure 1, the lung tissues of control group remained soft with a slightly pink appearance, while the lung tissues of LPS group showed congestive and swollen. Meanwhile, the lung tissues of OA group shrank and became stiff. Also, infarction-like dark area could be observed on its surface.

Histological evaluation and W/T ratio

The lower lobes of right lung were harvested at 15 minutes, 6 hours, 12 hours and 24 hours post-injection and they were used to evaluate the extent of the lesions. The results showed a significant histopathological change was observed in LPS and OA group when they were compared with control group at each time point ($p<0.05$, Figure 2A). Meanwhile, the scores of OA group were significantly higher than that of LPS group ($p<0.05$, Figure 2A), which was consistent with their appearance. Also, the left lungs were applied for W/D ratio analysis. As shown in Figure 2B, both LPS and OA administration

significantly increased W/D ratio at 6 hours after injection (p<0.05, Figure 2B), while no significant change was observed between LPS and OA administration (p>0.05, Figure 2B). At the mean time, there was no any notable change among three groups at 15 minutes, 12 hours and 24 hours post-injection (p>0.05, Figure 2B).

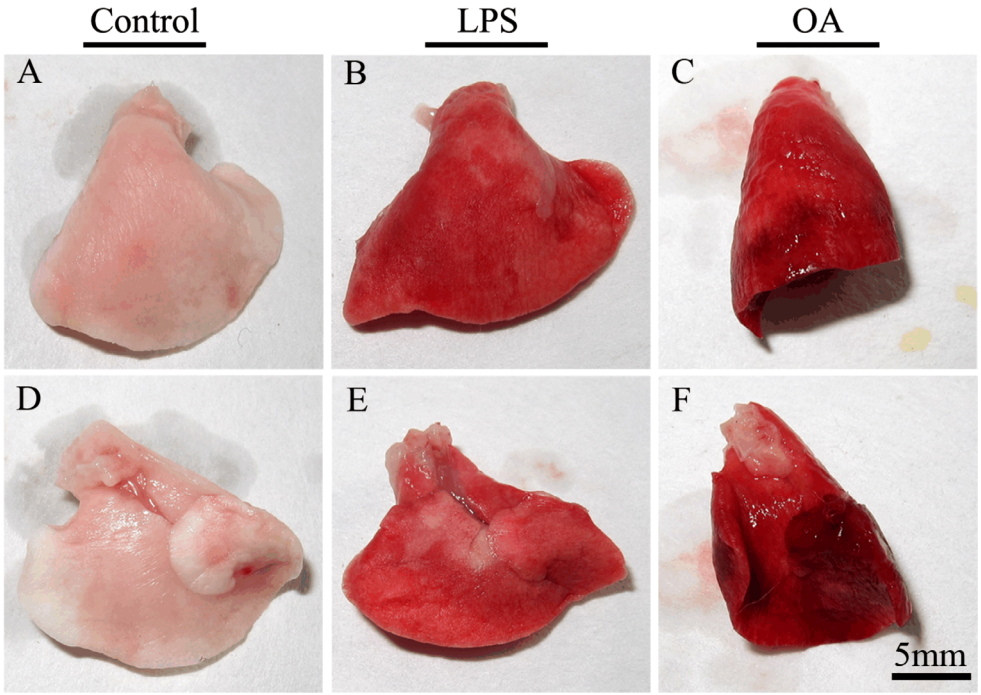

Figure 1 – ***Appearance change of lower lobes in right lungs: The dorsal views of the control group (A), LPS group (B) and OA group (C); The corresponding ventral views of the control group (D), LPS group (E) and OA group (F). Tissues were harvested at 6 hours after injection. Scale bar = 5 mm. LPS: Lipopolysaccharide; OA: Oleic acid.***

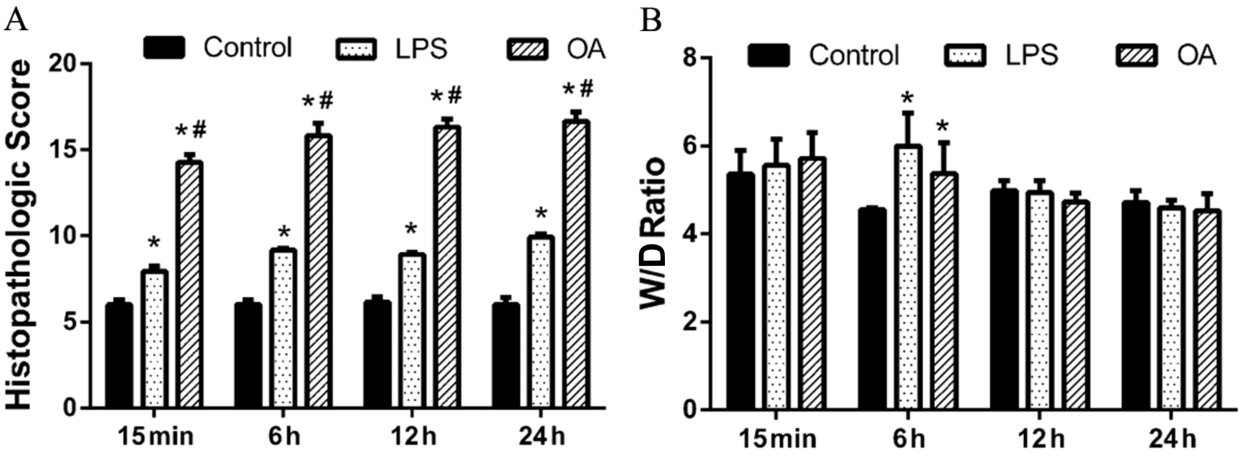

Figure 2 – ***The evaluation of lung injury and edema at different time point following injection: Histopathologic scores (A) and W/D ratio (B) among control, LPS and OA group (A). Lung injury was evaluated by a semi-quantitative scoring system. W/D ratio of left lung tissues was employed to assess pulmonary edema. Data were presented as means ± standard error of mean (SEM). Group comparisons were assessed by virtue of one-way analysis of variance (ANOVA): *p<0.05 compared with the control group and #p<0.05 compared with LPS group. W/D: Wet/Dry; LPS: Lipopolysaccharide; OA: Oleic acid.***

HE staining

In order to investigate the dynamic pathological manifestations, the lower lobes of right lung were applied for HE staining. The results showed that lung fields of the control group remained generally clear at all time points (Figure 3). In LPS groups, mild hemorrhage, leukocytes infiltration and edema could be observed in alveolar space at 15 minutes after LPS injection and lasted until 6 hours (Figure 3). At 12 hours after injection, hemorrhage and edema almost ceased, while leukocytes infiltration and alveolar wall thickening became the major pathological characteristics in the lung fields, which remained until 24 hours (Figure 3). Meanwhile, OA injection immediately induced severer and larger-scale hemorrhage in the lung accompanied with massive exudation and cavitation from 6 hours to 12 hours post-injection (Figure 3). Also, a large amount of leukocytes, thickened alveolar walls and hyaline membranes altogether formed a honeycomb-like structure in the lung, at 24 hours after injection (Figure 3).

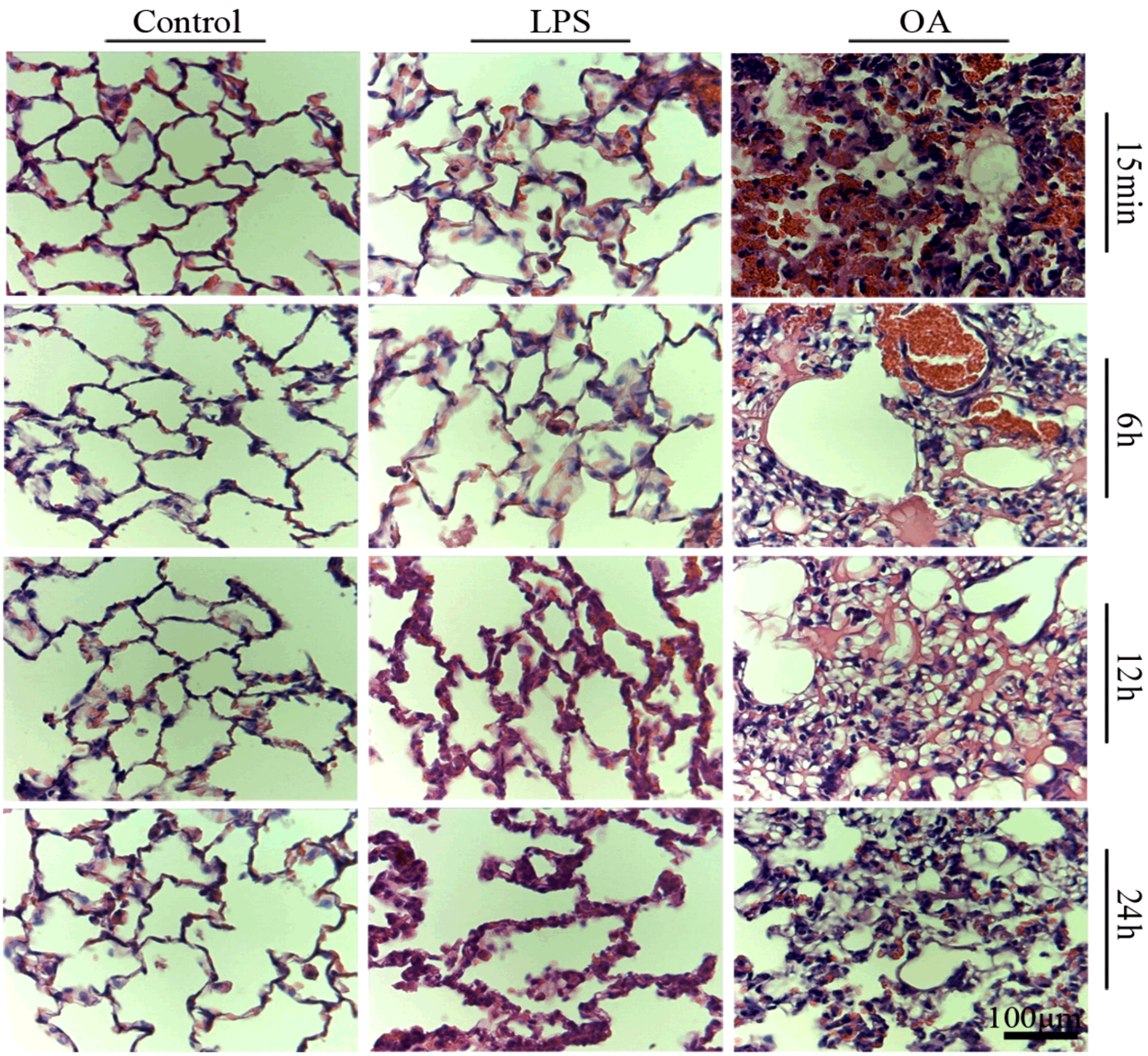

Figure 3 – ***Representative images of histopathologic changes: Images organized in columns according to their grouping and rows corresponding to the time points. Sections from lower lobe of right lung tissues were HE stained. Magnifications = 400×, scale bar = 100 μm. HE: Hematoxylin–Eosin; LPS: Lipopolysaccharide; OA: Oleic acid.***

Blood gas parameters

Four blood gas parameters were measured in this study. PaO_2 of LPS group exhibited no significant change compared to control group throughout the experiment ($p>0.05$, Figure 4A). However, PaO_2 of OA group dramatically decreased at 15 minutes after injection, compared with control group ($p>0.05$, Figure 4A). Then, the reduction lasted and significant difference was observed at 6 hours and 12 hours post-injection ($p<0.05$, Figure 4A), while recovered slightly at 24 hours ($p>0.05$, Figure 4A). Meanwhile, PaO_2 of OA group exhibited notably lower than LPS group from 15 minutes to 12 hours after injection ($p<0.05$, Figure 4A). Then, we measured the level of arterial carbon dioxide partial pressure ($PaCO_2$) and the results showed that three groups exhibited no significant differences at all time points ($p>0.05$, Figure 4B), except that $PaCO_2$ of OA group was much higher than that of LPS group, at 12 hours after injection ($p<0.05$, Figure 4B). The other acid–base balance indexes including LAC and buffer excess (BE) were also detected in the experiment. The result of LAC showed that a significant increase was observed in LPS and OA group when they were compared with control group, respectively, from 6 hours to 24 hours post-injection ($p<0.05$, Figure 4C). And the LAC level of OA group was much lower than LPS group at 12 hours ($p<0.05$, Figure 4C). Furthermore, the BE level of LPS group was significantly increased from 6 hours to 12 hours ($p<0.05$, Figure 4D) but recovered at 24 hours ($p>0.05$, Figure 4D) compared with control group. Also, the BE level of OA group showed a notable increase at 15 minutes, 6 hours, 24 hours ($p<0.05$, Figure 4D), while no significant change was observed at 12 hours compared to control group ($p>0.05$, Figure 4D). Additionally, OA group showed a lower BE level than LPS group at 12 hours post-injection ($p<0.05$, Figure 4D).

Biomarkers of blood–air barrier

Biomarkers of blood–air barrier (BAB) components were measured by real-time quantitative PCR. Both LPS and OA injection led to significantly increased mRNA level of advanced glycosylation end product-specific receptor

(AGER), the biomarker of type I alveolar epithelial cell (AECI) [9], at 6 hours after injection compared with control group (p<0.05, Figure 5A). Mucin 1 (MUC1), the biomarker of type II alveolar epithelial cell (AECII) [10], was only significantly upregulated in LPS group at 12 hours (p<0.05, Figure 5B) and was notably increased in OA group from 12 hours to 24 hours (p<0.05, Figure 5B) compared with control group. Furthermore, the MUC1 level of OA group was much lower than LPS group at 6 hours (p<0.05, Figure 5B) while began to increase from 12 hours (p>0.05, Figure 5B) and was much higher than LPS group at 24 hours (p<0.05, Figure 5B). OA injection immediately increased the level of von Willebrand factor (vWF), the biomarker of pulmonary vascular endothelial cells (PMVECs) [11], at 12 hours after injection (p<0.05, Figure 5C), while LPS injection increased the vWF level at 24 hours (p<0.05, Figure 5C). However, no significant difference was observed in laminin subunit alpha-5 (LAMA5) among the three groups, the biomarker of basement membranes (p>0.05, Figure 5D).

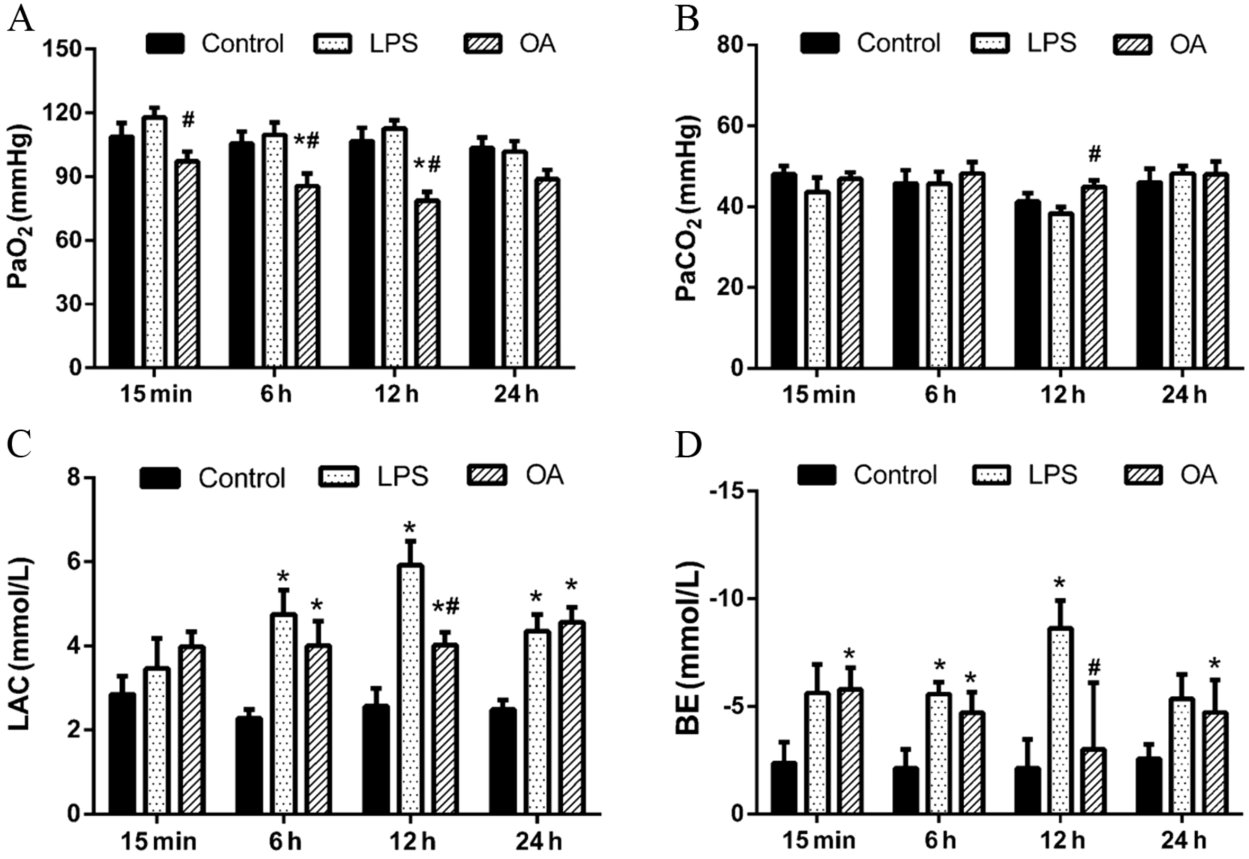

Figure 4 – ***Major blood gas parameters at different time point following injection: The level of PaO_2 (A), $PaCO_2$ (B), LAC (C) and BE (D). Data were presented as means ± standard error of mean (SEM). Group comparisons were assessed by virtue of one-way analysis of variance (ANOVA): *p<0.05 compared with control group and #p<0.05 compared with LPS group. LPS: Lipopolysaccharide; OA: Oleic acid; PaO_2: Arterial oxygen partial pressure; $PaCO_2$: Arterial carbon dioxide partial pressure); LAC: Lactic acid; BE: Buffer excess.***

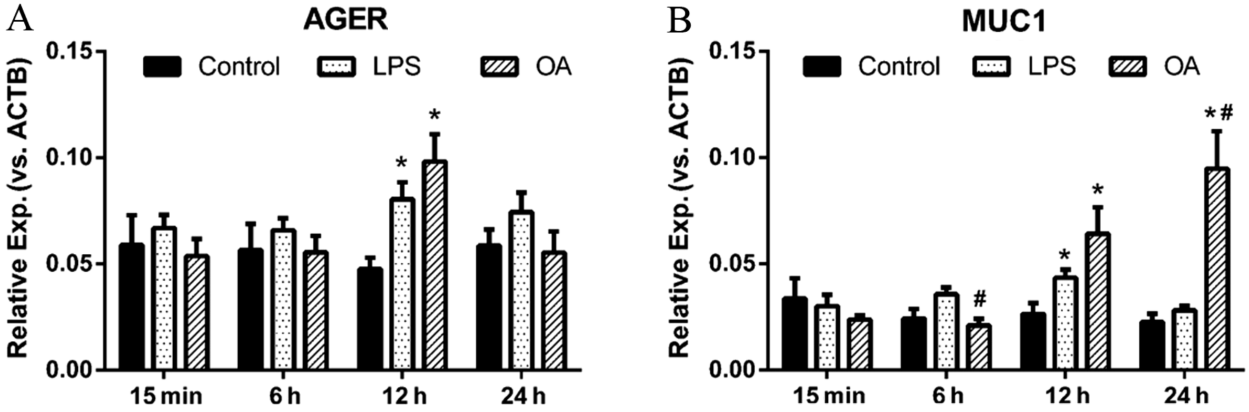

Figure 5 – ***The mRNA level of BAB components at different time point following injection: AGER (A), the biomarker of AECI; MUC1 (B), the biomarker of AECII. Data were presented as means ± standard error of mean (SEM). Group comparisons were assessed by virtue of one-way analysis of variance (ANOVA): *p<0.05 compared with control group and #p<0.05 compared with LPS group. AGER: Advanced glycosylation end product-specific receptor; MUC1: Mucin 1; LPS: Lipopolysaccharide; OA: Oleic acid; ACTB: β-Actin gene; mRNA: Messenger ribonucleic acid; BAB: Blood–air barrier; AECI: Type I alveolar epithelial cell; AECII: Type II alveolar epithelial cell.***

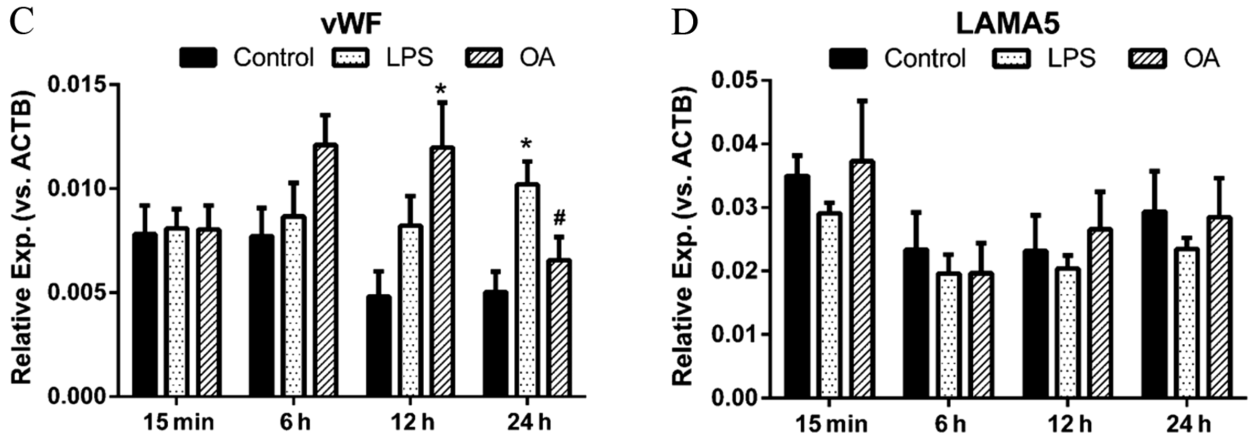

Figure 5 (continued) – ***The mRNA level of BAB components at different time point following injection: vWF (C), the biomarker of PMVECs; LAMA5 (D), the biomarker of basement membranes. Data were presented as means ± standard error of mean (SEM). Group comparisons were assessed by virtue of one-way analysis of variance (ANOVA): *p<0.05 compared with control group and #p<0.05 compared with LPS group. vWF: von Willebrand factor; LAMA5: Laminin subunit alpha-5; LPS: Lipopolysaccharide; OA: Oleic acid; ACTB: β-Actin gene; mRNA: Messenger ribonucleic acid; BAB: Blood–air barrier; PMVECs: Pulmonary vascular endothelial cells.***

Discussion

In this research, we applied histological evaluation, W/D ratio, blood gas parameters and biomarkers of BAB to explain the difference existed between the OA-induced model and LPS-induced model of rats. We found OA injection had a more serious histological injury than LPS injection including obvious hemorrhage, massive exudation, leukocytes infiltration. Also, LPS injury had no influence on the level of PaO_2 as OA infusion did. And profiles of BAB component biomarkers in each model were unique.

Several reasons may account for this. Firstly, mechanism of OA-induced lung injury is initialized by its direct impairment to the PMVECs *via* oxidative stress [12], and then other inflammatory factors involved in this procedure serve as subsequent events [13], suggesting that OA-induced model is not dependent on the inflammatory reaction. In contrast, as glycolipid used in membrane of Gram-negative bacteria, LPS binding to a specific LPS binding protein (LBP) forms an LPS:LBP complex that activates the CD14/Toll-like receptor-4 (TLR4) receptor of monocytes, macrophages, and other cells, triggering the production of inflammatory mediators [14]. Besides, as a macromolecular substance, OA was carried into right heart and pulmonary circulation by bloodstream after injection, and then was detained in the alveoli, while the LPS:LBP complex remained in bloodstream to trigger the systemic inflammatory response, which may explain the higher LAC level of the LPS group which is associated with a severe microcirculatory disturbance. Though other studies reported that intravenous injection of LPS managed to decrease PaO_2 [15, 16], application of conclusion from rat model to human still calls for considerable caution.

The BAB is the anatomical and physiological basis of gas exchange in lung. Each component of BAB has its unique function. For example, AECI and PMVECs form the semi-permeable barrier between the vascular and alveolar spaces with matrix. AECII secrets surfactant and differentiates into AECI to repair the barrier [17]. In our study, the OA injection caused earlier and greater changes in the biomarkers of most BAB components, while the mild effects of LPS challenge on the biomarkers emerged later. This finding indicates that this difference should be taken into consideration in designing study of ALI *in vitro*.

Discrepancy between animal models and real clinical cases weighs more than the difference between models. Unlike the human ALI patients, ALI model rats in this investigation had shorter course of disease and more mildly reduced PaO_2, in particular, no decrease of PaO_2 was observed in the LPS groups. Zhou *et al.* reported similar phenomenon [18] that a single dosage of LPS has no effect on PaO_2 in rats. Besides, the typical exudative phase of human ALI patients usually lasts for one or two days [19] followed by a fibro-proliferative phase from day 3 to day 7, while exudation of most rats in this study was absorbed within 24 hours and fibro-proliferation became the major morphological change subsequently. This difference implied that rats boast stronger tolerance and restorability to endotoxin than human, which may arise from two aspects. Firstly, rats and humans display 10 amino acid differences in the TLR4 Toll/interleukin-1 receptor (TIR) domain out of 169 amino acids [20], so rats have lower sensitivity to LPS than human. Additionally, human and rodent macrophages differ significantly in their ability to produce nitric oxide (NO). Rodent macrophages produce larger amounts of NO than normal non-activated human macrophages do [8]. Yoshikawa *et al.* reported that NO played a protective role in the acute lung injury and mortality induced by the platelet-activating factor [21].

An ideal animal model of ALI should reproduce the mechanisms and consequences of ALI in humans, including the physiological and pathological changes. Nevertheless, no single animal model could satisfy this need due to the multiple initial events of real ALI cases. Studies of multiple stimulants [5] or "second-hit" injury models [22] may boast greater similarity to human ALI patients.

Conclusions

Two rat models of ALI were different in terms of pathological features, blood gas manifestation and BAB impairments. Moreover, LPS-induced model has greater value based on researches of microcirculation dysfunction

and sepsis resulting from ALI, while OA-induced model has greater repeatability in the area of gas exchanging after ALI. This study is the first time to quantitatively analyze the difference, which may provide a precise choice for the model of ALI/acute respiratory distress syndrome (ARDS).

Conflict of interests

All authors declare no relationships that could be construed as a conflict of interests.

Acknowledgments

We sincerely thank Feifei Shang, PhD from Institute of Life Sciences, Chongqing Medical University, China, for making substantial contributions to analysis and the experimental technical guidance.

Author contribution

Yuan-Dong Hu and Ling Jiang contributed equally to this work.

(I) Conception and design: Ting-Hua Wang, Yuan-Dong Hu and Ling Jiang; (II) Administrative support: Ting-Hua Wang and Qing-Jie Xia; (III) Provision of study materials or patients: Yuan-Dong Hu; (IV) Collection and assembly of data: Yuan-Dong Hu and Ling Jiang; (V) Data analysis and interpretation: Yue Hu and Liu-Lin Xiong; (VI) Manuscript writing: All authors; (VII) Final approval of manuscript: All authors.

References

[1] Imam F, Al-Harbi NO, Al-Harbi MM, Ansari MA, Zoheir KM, Iqbal M, Anwer MK, Al Hoshani AR, Attia SM, Ahmad SF. Diosmin downregulates the expression of T cell receptors, pro-inflammatory cytokines and NF-κB activation against LPS-induced acute lung injury in mice. Pharmacol Res, 2015, 102:1–11.

[2] Calfee CS, Matthay MA. Nonventilatory treatments for acute lung injury and ARDS. Chest, 2007, 131(3):913–920.

[3] Matute-Bello G, Frevert CW, Martin TR. Animal models of acute lung injury. Am J Physiol Lung Cell Mol Physiol, 2008, 295(3):L379–L399.

[4] Jesmin S, Zaedi S, Islam AM, Sultana SN, Iwashima Y, Wada T, Yamaguchi N, Hiroe M, Gando S. Time-dependent alterations of VEGF and its signaling molecules in acute lung injury in a rat model of sepsis. Inflammation, 2012, 35(2): 484–500.

[5] Pfeifer R, Andruszkow JH, Busch D, Hoepken M, Barkatali BM, Horst K, Pape HC, Hildebrand F. Development of a standardized trauma-related lung injury model. J Surg Res, 2015, 196(2):388–394.

[6] ARDS Definition Task Force, Ranieri VM, Rubenfeld GD, Thompson BT, Ferguson ND, Caldwell E, Fan E, Camporota L, Slutsky AS. Acute respiratory distress syndrome: the Berlin Definition. JAMA, 2012, 307(23):2526–2533.

[7] Li T, Cai S, Zeng Z, Zhang J, Gao Y, Wang X, Chen Z. Protective effect of polydatin against burn-induced lung injury in rats. Respir Care, 2014, 59(9):1412–1421.

[8] Breithaupt-Faloppa AC, Vitoretti LB, Coelho FR, dos Santos Franco AL, Domingos HV, Sudo-Hayashi LS, Oliveira-Filho RM, Tavares de Lima W. Nitric oxide mediates lung vascular permeability and lymph-borne IL-6 after an intestinal ischemic insult. Shock, 2009, 32(1):55–61.

[9] Briot R, Frank JA, Uchida T, Lee JW, Calfee CS, Matthay MA. Elevated levels of the receptor for advanced glycation end products, a marker of alveolar epithelial type I cell injury, predict impaired alveolar fluid clearance in isolated perfused human lungs. Chest, 2009, 135(2):269–275.

[10] Ishizaka A, Matsuda T, Albertine KH, Koh H, Tasaka S, Hasegawa N, Kohno N, Kotani T, Morisaki H, Takeda J, Nakamura M, Fang X, Martin TR, Matthay MA, Hashimoto S. Elevation of KL-6, a lung epithelial cell marker, in plasma and epithelial lining fluid in acute respiratory distress syndrome. Am J Physiol Lung Cell Mol Physiol, 2004, 286(6):L1088–L1094.

[11] Qian JX, Lu SQ, Zhao YM, Lu JH. Expression patterns of plasma von Willebrand factor and serum interleukin-8 in patients with early-stage severe pulmonary contusion. World J Emerg Med, 2011, 2(2):122–126.

[12] Yang C, Moriuchi H, Takase J, Ishitsuka Y, Irikura M, Irie T. Oxidative stress in early stage of acute lung injury induced with oleic acid in guinea pigs. Biol Pharm Bull, 2003, 26(4): 424–428.

[13] Inoue H, Nakagawa Y, Ikemura M, Usugi E, Nata M. Molecular-biological analysis of acute lung injury (ALI) induced by heat exposure and/or intravenous administration of oleic acid. Leg Med (Tokyo), 2012, 14(6):304–308.

[14] Tapping RI, Akashi S, Miyake K, Godowski PJ, Tobias PS. Toll-like receptor 4, but not Toll-like receptor 2, is a signaling receptor for *Escherichia* and *Salmonella* lipopolysaccharides. J Immunol, 2000, 165(10):5780–5787.

[15] Gao J, Zhan Y, Chen J, Wang L, Yang J. Triptolide ameliorates lipopolysaccharide-induced acute lung injury in rats. Eur J Med Res, 2013, 18:58.

[16] Han G, Ma L, Guo Y, Li L, Li D, Liu H. Hyperbaric oxygen therapy palliates lipopolysaccharide-induced acute lung injury in rats by upregulating AQP1 and AQP5 expression. Exp Lung Res, 2015, 41(8):444–449.

[17] Sapru A, Flori H, Quasney MW, Dahmer MK; Pediatric Acute Lung Injury Consensus Conference Group. Pathobiology of acute respiratory distress syndrome. Pediatr Crit Care Med, 2015, 16(5 Suppl 1):S6–S22.

[18] Zhou GJ, Jiang SY, Zhang M, Gan JX, Jiang GY. Evaluation of the inflammatory response in a two-hit acute lung injury model using [18F]FDG microPET. Exp Ther Med, 2013, 6(4): 894–898.

[19] Tomashefski JF Jr. Pulmonary pathology of the adult respiratory distress syndrome. Clin Chest Med, 1990, 11(4):593–619.

[20] Sanghavi SK, Shankarappa R, Reinhart TA. Genetic analysis of Toll/interleukin-1 receptor (TIR) domain sequences from *Rhesus* macaque Toll-like receptors (TLRs) 1-10 reveals high homology to human TLR/TIR sequences. Immunogenetics, 2004, 56(9):667–674.

[21] Yoshikawa T, Takano H, Yamamoto H, Nakahashi Y, Yamaguchi T, Arimoto T, Kondo M. Role of superoxide and nitric oxide in platelet-activating factor-induced acute lung injury, hypotension, and mortality in rats. Crit Care Med, 1997, 25(2): 286–292.

[22] Pan C, Wang J, Liu W, Liu L, Jing L, Yang Y, Qiu H. Low tidal volume protects pulmonary vasomotor function from "second-hit" injury in acute lung injury rats. Respir Res, 2012, 13:77.

Corresponding author

Ting-Hua Wang, Professor, MD, PhD, Department of Anesthesiology, West China Hospital, Sichuan University, Chengdu, China; Institute of Neurological Disease, West China Hospital, Sichuan University, Wuhou District of Chengdu, Sichuan Province, People's South Road, Block 3, No. 17, Chengdu, China; Phone 18227648857, Fax +86-28-85501036, e-mail: tinghua_neuron@263.net

Received: July 1, 2017 *Accepted: January 18, 2018*